THE JOURNAL OF BIOLOGICAL CHEMISTRY VOL. 291, NO. 37, pp. 19687–19700, September 9, 2016

Cardiac Myocyte-specific Knock-out of Calcium-independent Phospholipase $A_2\gamma$ ($iPLA_2\gamma$) Decreases Oxidized Fatty Acids during Ischemia/Reperfusion and Reduces Infarct Size*

Received for publication, May 26, 2016, and in revised form, July 22, 2016 Published, JBC Papers in Press, July 23, 2016, DOI 10.1074/jbc.M116.740597

Sung Ho Moon[‡], David J. Mancuso[‡], Harold F. Sims[‡], Xinping Liu[‡], Annie L. Nguyen[§1], Kui Yang[‡], Shaoping Guan[‡], Beverly Gibson Dilthey[‡], Christopher M. Jenkins[‡], Carla J. Weinheimer[§], Attila Kovacs[§], Dana Abendschein[§], and Richard W. Gross[‡§¶‖2]

From the [‡]Division of Bioorganic Chemistry and Molecular Pharmacology, Departments of Medicine, [¶]Developmental Biology, and [§]Center for Cardiovascular Research, Washington University School of Medicine, Saint Louis, Missouri 63110 and the [‖]Department of Chemistry, Washington University, Saint Louis, Missouri 63130

Calcium-independent phospholipase $A_2\gamma$ ($iPLA_2\gamma$) is a mitochondrial enzyme that produces lipid second messengers that facilitate opening of the mitochondrial permeability transition pore (mPTP) and contribute to the production of oxidized fatty acids in myocardium. To specifically identify the roles of $iPLA_2\gamma$ in cardiac myocytes, we generated cardiac myocyte-specific $iPLA_2\gamma$ knock-out ($CMiPLA_2\gamma KO$) mice by removing the exon encoding the active site serine (Ser-477). Hearts of $CMiPLA_2\gamma KO$ mice exhibited normal hemodynamic function, glycerophospholipid molecular species composition, and normal rates of mitochondrial respiration and ATP production. In contrast, $CMiPLA_2\gamma KO$ mice demonstrated attenuated Ca^{2+}-induced mPTP opening that could be rapidly restored by the addition of palmitate and substantially reduced production of oxidized polyunsaturated fatty acids (PUFAs). Furthermore, myocardial ischemia/reperfusion (I/R) in $CMiPLA_2\gamma KO$ mice (30 min of ischemia followed by 30 min of reperfusion *in vivo*) dramatically decreased oxidized fatty acid production in the ischemic border zones. Moreover, $CMiPLA_2\gamma KO$ mice subjected to 30 min of ischemia followed by 24 h of reperfusion *in vivo* developed substantially less cardiac necrosis in the area-at-risk in comparison with their WT littermates. Furthermore, we found that membrane depolarization in murine heart mitochondria was sensitized to Ca^{2+} by the presence of oxidized PUFAs. Because mitochondrial membrane depolarization and calcium are known to activate $iPLA_2\gamma$, these results are consistent with salvage of myocardium after I/R by $iPLA_2\gamma$ loss of function through decreasing mPTP opening, diminishing production of proinflammatory oxidized fatty acids, and attenuating the deleterious effects of abrupt increases in calcium ion on membrane potential during reperfusion.

The salvage of jeopardized regions of myocardium during ischemia/reperfusion (I/R)[3] has been a long-standing goal of heart research. Because mortality and morbidity are related to infarct size, a variety of hemodynamic, metabolic, and pharmacological approaches have been used to reduce the severity of myocardial infarction during ischemia (1–3). Recent studies have accumulated evidence that the irreversible opening of the mitochondrial permeability transition pore (mPTP) upon oxidative stress is a principal mechanism of apoptotic/necrotic cardiac cell death accounting for the majority of I/R injury (4–6). Although therapies for acute ischemia (*e.g.* reperfusion) have been extensively studied, at present there is no therapy for attenuating mPTP opening during reperfusion of ischemic zones in myocardium.

Although the precise chemical composition of the mPTP is incompletely understood (6), a variety of initiators and modulators of mPTP opening has been identified (7, 8). For example, during reperfusion, the reoxygenation of ischemic tissue results in mitochondrial Ca^{2+} overload and renormalization of intracellular and matrix pH, which are accompanied by the prodigious generation of reactive oxygen species that synergistically induce the opening of the mPTP. Furthermore, both fatty acids and their acyl-CoA derivatives increase dramatically during myocardial ischemia and each greatly facilitate mPTP opening (9–15). The extensive permeability of the inner mitochondrial membrane culminates in the release of proapoptotic factors and the efflux of toxic lipid metabolites into the cytosol that collectively precipitate irreversible myocardial necrosis and apoptosis (10, 16, 17).

Previously, we identified a novel calcium-independent phospholipase $A_2\gamma$ ($iPLA_2\gamma$; also known as PNPLA8) that was membrane-associated, present in multiple tissues, and possessed

* This work was supported by National Institutes of Health Grant RO1HL118639 (to R. W. G.). R. W. G. has financial relationships with LipoSpectrum and Platomics. The content is solely the responsibility of the authors and does not necessarily represent the official views of the National Institutes of Health.

[1] Present address: Dept. of Neurology, Washington University School of Medicine, Saint Louis, MO 63110.

[2] To whom correspondence should be addressed: Division of Bioorganic Chemistry and Molecular Pharmacology, Washington University School of Medicine, 660 S. Euclid Ave., Campus Box 8020, St. Louis, MO 63110. Tel.: 314-362-2690; Fax: 314-362-1402; E-mail: rgross@wustl.edu.

[3] The abbreviations used are: I/R, ischemia/reperfusion; CL, cardiolipin; $CMiPLA_2\gamma KO$, cardiac myocyte-specific $iPLA_2\gamma$ knock-out; EET, epoxyeicosatrienoic acid; FLP, flippase; HDoHE, hydroxydocosahexaenoic acid; HETE, hydroxyeicosatetraenoic acid; $iPLA_2\gamma$, calcium-independent phospholipase $A_2\gamma$; mPTP, mitochondrial permeability transition pore; oxoODE, oxo-octadecadienoic acid; PG, prostaglandin; I.S., internal standard; oxlam, oxidized linoleic acid metabolite; FCCP, trifluoromethoxy carbonylcyanide phenylhydrazone; MRM, multiple reaction monitoring; AMPP, *N*-(4-aminomethylphenyl) pyridinium; TTC, triphenyltetrazolium chloride; D, diacyl; TPP^+, tetraphenylphosphonium; LAD, left anterior descending; FRT, flippase recombinase target; MDMS-SL, multidimensional mass spectrometry-based shotgun lipidomics.

multiple discrete isoforms (18). Further studies demonstrated that iPLA$_2$γ transcription was tightly regulated through multiple complex mechanisms (19). Through immunohistochemistry and cardiac myocyte-specific expression, iPLA$_2$γ was shown to be localized to mitochondrial and peroxisomal compartments. Transgenic expression of iPLA$_2$γ resulted in the dramatic increase of 2-arachidonoyl lysophosphatidylcholine and 2-docosahexaenoyl lysophosphatidylcholine in cardiac myocytes (19, 20). Later studies also identified iPLA$_2$γ in the endoplasmic reticulum (21). To begin the mechanistic dissection of the roles of iPLA$_2$γ in biological function in health and disease, we generated a germ line knock-out of iPLA$_2$γ in mice (iPLA$_2$γ KO) (22–24). These studies revealed that iPLA$_2$γ loss of function dramatically reduced the opening of the mitochondrial permeability transition pore (mPTP) in liver mitochondria and that calcium challenge of myocardial mitochondria obtained from the iPLA$_2$γ KO mouse markedly decreased the production of inflammatory eicosanoids in comparison with wild-type mice. However, germ line iPLA$_2$γ KO mice displayed multiple defects in virtually every organ system studied, thus rendering definitive mechanistic interpretation of responses to *in vivo* cardiac ischemia difficult. To traverse this difficulty, in this study we generated cardiac myocyte-specific iPLA$_2$γ knock-out mice (CMiPLA$_2$γKO) by inserting flox sites proximal and distal to the active site serine of iPLA$_2$γ (Ser-477 in exon 5) and subsequently excising the exon containing the active site by tamoxifen-activated cardiac myocyte-specific Cre recombinase. Utilizing this novel genetic mouse model, we have investigated the effects of cardiac myocyte-specific KO of iPLA$_2$γ on ischemia/reperfusion *in vivo*.

The regiospecificity of iPLA$_2$γ toward phospholipid substrates is atypical among mammalian PLA$_2$ enzymes in that the site of hydrolysis is dependent on the nature of the *sn*-2 aliphatic group (25). Specifically, if the *sn*-2 group is saturated or contains a single double bond, iPLA$_2$γ exhibits no preference for cleavage of the fatty acyl group at the *sn*-1 or *sn*-2 position. In sharp contrast, if the *sn*-2 substituent is polyunsaturated, iPLA$_2$γ serves predominantly as a PLA$_1$ releasing the saturated fatty acid from the *sn*-1 position and generating 2-polyunsaturated fatty acyl lysolipids. Thus, the regiospecificity of hydrolysis is determined by the degree of unsaturation in the *sn*-2 phospholipid constituent. This unusual feature allows the enzyme to accomplish multiple regulatory functions in mitochondria, including the release of palmitate in the inner membrane, which opens the mPTP, the generation of polyunsaturated lysophospholipids, which are readily hydrolyzed by endogenous lipases to lead to the production of bioactive oxidized fatty acids (*e.g.* eicosanoids, docosanoids, etc.), and the provision of fatty acid substrates for use in mitochondrial energy generation.

Accordingly, we hypothesized that loss of cardiac iPLA$_2$γ function would decrease I/R injury through a four-tiered synergistic mechanism involving the following: 1) attenuation of mPTP opening; 2) decreased inflammatory lipid second messengers; 3) preservation of mitochondrial membrane potential; and 4) attenuated release of toxic lipid metabolites (*e.g.* nonesterified saturated fatty acids, lysolipids, acyl-CoAs, and acylcarnitines) that accumulate during myocardial ischemia and are released during reperfusion.

In this study, we utilized CMiPLA$_2$γKO mice to investigate iPLA$_2$γ-mediated mPTP opening upon calcium challenge, its role in the production of proinflammatory lipid metabolites (eicosanoids, docosanoids, and oxidized linoleic acid metabolites) in the border zone, and the development of cardiac necrosis after I/R in the absence of the confounding pathologies that were present in the germ line knock-out. Importantly, we demonstrate that myocardial loss of iPLA$_2$γ function substantially reduces infarct size after I/R *in vivo* and markedly decreases production of inflammatory oxidized fatty acids (oxylipins) in the ischemic border zone. Through ablation of iPLA$_2$γ-facilitated mPTP opening, generation of inflammatory lipid second messengers, and the release of toxic mitochondrial metabolites, a novel strategy to attenuate cardiac necrosis and inflammation during acute coronary syndromes has been identified.

Results

Generation of Cardiac Myocyte-specific iPLA$_2$γ Knock-out Mice—To definitively identify the mechanistic importance of iPLA$_2$γ in cardiac myocytes, we engineered an inducible cardiac myocyte-specific knock-out of iPLA$_2$γ. Because of the presence of multiple transcriptional start sites in iPLA$_2$γ, our strategy was to flox exon 5 containing the active site and remove it by tamoxifen induction of cardiac myocyte-specific Cre recombinase (Fig. 1). Southern analysis for the floxed iPLA$_2$γ allele in multiple tissues of the f/f mouse and PCR analyses for the identification of ablation of the PGK-neo cassette and iPLA$_2$γ$^{f/f}$ Cre$^+$ in the iPLA$_2$γ conditional KO mice are shown in Fig. 1. Northern and Western analyses demonstrated the specific ablation of iPLA$_2$γ in heart but not in other tissues in the CMiPLA$_2$γKO mouse (Fig. 1, *E* and *F*).

Demonstration That the Majority of iPLA$_2$γ Activity in Myocardium Is Present in Cardiac Myocytes and Discrete Tissue Distributions of iPLA$_2$γ Isoforms in Different Tissues—Myocardium is composed of multiple cell types, including cardiac myocytes, endothelial cells, smooth muscle cells, fibroblasts, and macrophages. Although myocardium contains substantial amounts of iPLA$_2$γ activity and protein, the cell type of origin of iPLA$_2$γ is not known with certainty. Comparisons of WT Cre$^+$ with CMiPLA$_2$γKO mice definitively demonstrate that the overwhelming majority of iPLA$_2$γ protein of murine myocardium is present in cardiac myocytes by tissue-specific knockout mediated by the specificity of cardiac myocyte-specific expression of Cre recombinase. Moreover, the results of Fig. 1*F* demonstrate the diverse tissue-specific distribution of iPLA$_2$γ isoforms (*e.g.* 88, 74, 63, and 52 kDa), which were previously identified by germ line knock-out and transgenic overexpression of iPLA$_2$γ (9, 19, 20). For example, note the predominance of the lower molecular mass iPLA$_2$γ isoforms (50–60 kDa) in liver in comparison with myocardium and brain. Collectively, these results demonstrate that iPLA$_2$γ in myocardium is predominantly located in cardiac myocytes and identify the tissue-specific distributions of different isoforms of iPLA$_2$γ.

Constitutional Characteristics of the CMiPLA$_2$γKO Mouse—In contrast to the global iPLA$_2$γ knock-out, which demonstrated a thin body habitus, decreased length, cognitive dysfunction, kyphosis, and decreased locomotor activity (22, 24), the CMiPLA$_2$γKO mice gained weight normally, possessed

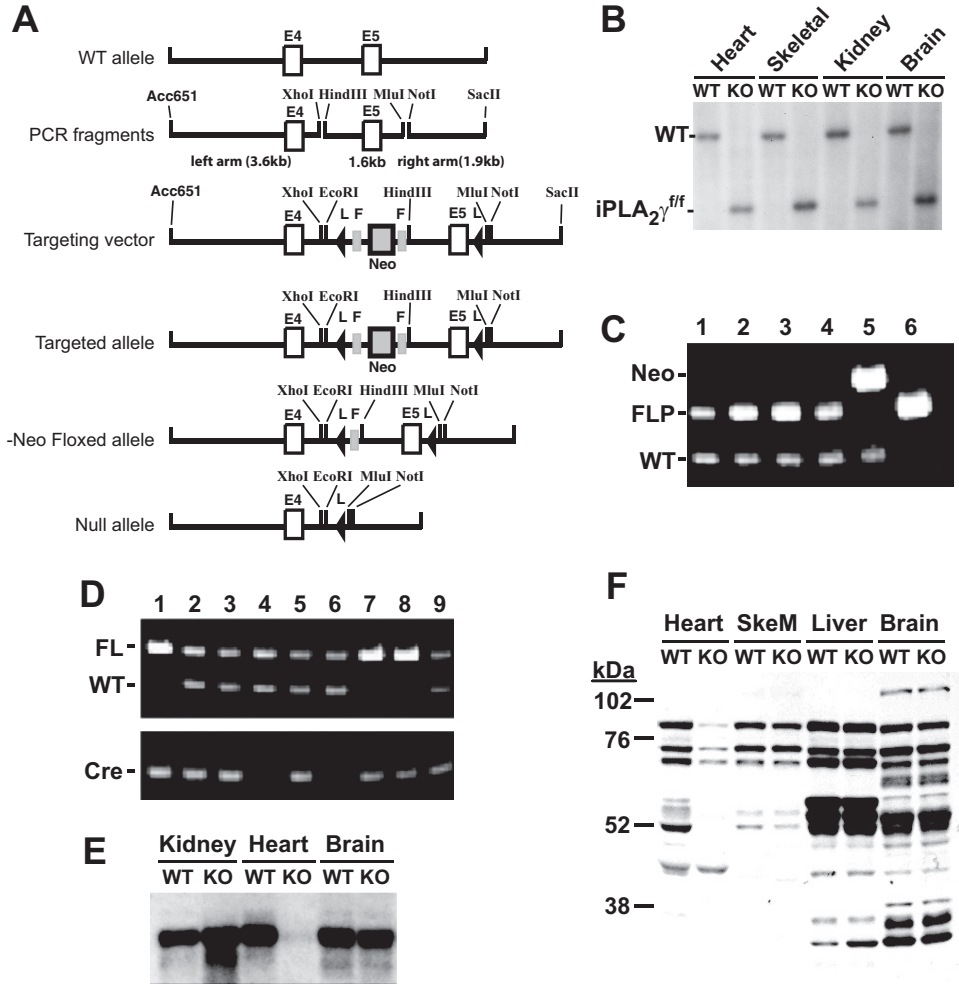

FIGURE 1. **Cardiac myocyte-specific ablation of iPLA$_2\gamma$ in mouse myocardium.** *A,* graphic representation of the iPLA$_2\gamma$ conditional targeting strategy. Exons 4 and 5 (*E4, E5*) of the WT allele are depicted as *open boxes,* and the intronic sequence is represented as a *solid line*. PCR products generated for construction of the targeting construct with restriction sites used for cloning are as indicated. The targeting vector is shown with FLP sites (*F*) indicated as *closed boxes* flanking the PGK-neo cassette and loxP sites indicated as *triangle* (*L*) flanking both the PGK-neo cassette (*Neo*) and E5. Below the targeting vector is a representation of the targeted allele in the conditional KO mouse. Breeding this mouse with an FLP recombinase mouse results in ablation of the PGK-neo cassette, generating the floxed allele. Finally, breeding with the Cre mouse results in ablation of E5, and the generation of the null allele is represented at the bottom. *B,* genomic Southern analysis of wild-type (*WT*) and Neo iPLA$_2\gamma^{f/f}$ mice shows the presence of only floxed iPLA$_2\gamma$ alleles in multiple tissues of the f/f mouse. *C,* successful ablation of the PGK-neo cassette in the iPLA$_2\gamma$ conditional KO mouse. PCR analysis of tail DNA was utilized to identify mice from which the PGK-neo cassette had been ablated by crossing the conditional knock-out with a global FLP mouse. *Lanes 1–4* identify heterozygous mice lacking the PGK-neo (*Neo*) cassette but have the floxed and WT alleles (iPLA$_2\gamma^{f/+}$). *Lane 5* identifies a heterozygous mouse having the PGK-neo allele (*Neo*). A mouse homozygous for the floxed allele was identified in *lane 6* (iPLA$_2\gamma^{f/f}$). *D,* PCR identification of heart-specific conditional KO Cre$^+$ mice. Tail PCR amplification of floxed (*FL*) and WT alleles along with Cre transgene (*Cre*) expression was used to identify iPLA$_2\gamma^{f/+}$ Cre$^+$ (*lanes 2, 3, 5,* and *9*) and iPLA$_2\gamma^{f/f}$ Cre$^+$ (*lanes 1, 7,* and *8*) mice. *E,* Northern analysis of RNA isolated from heart, kidney and brain of WT and CMiPLA$_2\gamma$KO (*KO*) mice. The results demonstrate the tissue-specific ablation of iPLA$_2\gamma$ in heart but not kidney or brain of the conditional knock-out. *F,* Western analysis of iPLA$_2\gamma$ expression in WT and CMiPLA$_2\gamma$KO (KO) tissues. Lanes: *heart*, skeletal muscle (*SkeM*), *liver,* and brain.

normal insulin sensitivity, did not develop kyphosis, and had no demonstrable sensory-motor abnormalities (data not shown).

Echocardiographic analyses of myocardial hemodynamic function in the CMiPLA$_2\gamma$KO mice at 6 months of age (3 months after tamoxifen administration) revealed no significant alterations in left ventricular wall thickness, left ventricular mass index, or chamber diameters during end systole/diastole and displayed normal fractional shortening in comparison with WT littermates (Table 1).

High Resolution Respirometry of Myocardial Mitochondria from WT and CMiPLA$_2\gamma$KO Mice—High resolution respirometry of myocardial mitochondria was performed to identify alterations in mitochondrial function and respiratory coupling efficiency in CMiPLA$_2\gamma$KO mice. To examine mitochondrial bioenergetic efficiency under different conditions, we utilized multiple substrates, including pyruvate/malate, palmitoylcarnitine/malate, and pyruvate/glutamate/malate. Mitochondria from CMiPLA$_2\gamma$KO mice demonstrated similar oxygen consumption rates in comparison with WT littermates during both state 2 and 3 respiration or after inhibition of complex I (rotenone) or complex V (oligomycin-induced state 4) (Fig. 2). The coupling of electron transport to oxidative phosphorylation (P/O ratio), which was determined by quantifying ATP production and O_2 consumption during state 3 respiration, was not significantly different in WT *versus* CMiPLA$_2\gamma$KO mice (Fig. 2). These results demonstrate the ability of mitochondria from the CMiPLA$_2\gamma$KO to respire normally and efficiently synthesize ATP.

TABLE 1

Echocardiographic analysis of myocardial hemodynamic function in wild-type (WT) and cardiac myocyte-specific iPLA$_2\gamma$ knock-out (KO) mice under light anesthesia

Echocardiographic comparisons of hemodynamic function in WT Cre$^+$ *versus* CMiPLA$_2\gamma$KO mice at 6 months of age demonstrated no alterations in cardiac function after cardiac myocyte genetic ablation of iPLA$_2\gamma$. Parameters examined for each group were as follows: HR, heart rate (beats/min); LVPWd, left ventricular posterior wall thickness at end diastole (mm); IVSd, interventricular septal wall thickness at end diastole (mm); LVIDd, left ventricular internal diameter at end diastole (mm); LVPW, LV posterior wall thickness at end systole (mm); IVS, interventricular septal wall thickness at end systole (mm); LVID, LV internal diameter at end systole (mm); LVM, left ventricular mass (mg); RWT, relative wall thickness; FS, fractional shortening (%). Data are presented as the mean ±S.D.utilizing six WT and six CMiPLA$_2\gamma$KO male mice.

Type	Body wt	HR	LVPWd	IVSd	LVIDd	LVPW	IVS	LVID	LVM	LVMI	RWT	FS
	g	*beats/min*	*mm*	*mm*	*mm*	*mm*	*mm*	*mm*	*mg*			*%*
WT	30.3±1.7	638.7±51.8	0.93±0.06	0.99±0.04	3.59±0.25	1.56±0.20	1.67±0.14	1.60±0.20	124.7±9.4	4.12±0.28	0.54±0.05	55.3±5.0
KO	31.2±2.9	651.0±11.8	0.95±0.06	0.96±0.03	3.72±0.25	1.63±0.14	1.68±0.12	1.59±0.24	131.1±7.6	4.22±0.34	0.51±0.06	57.2±4.9

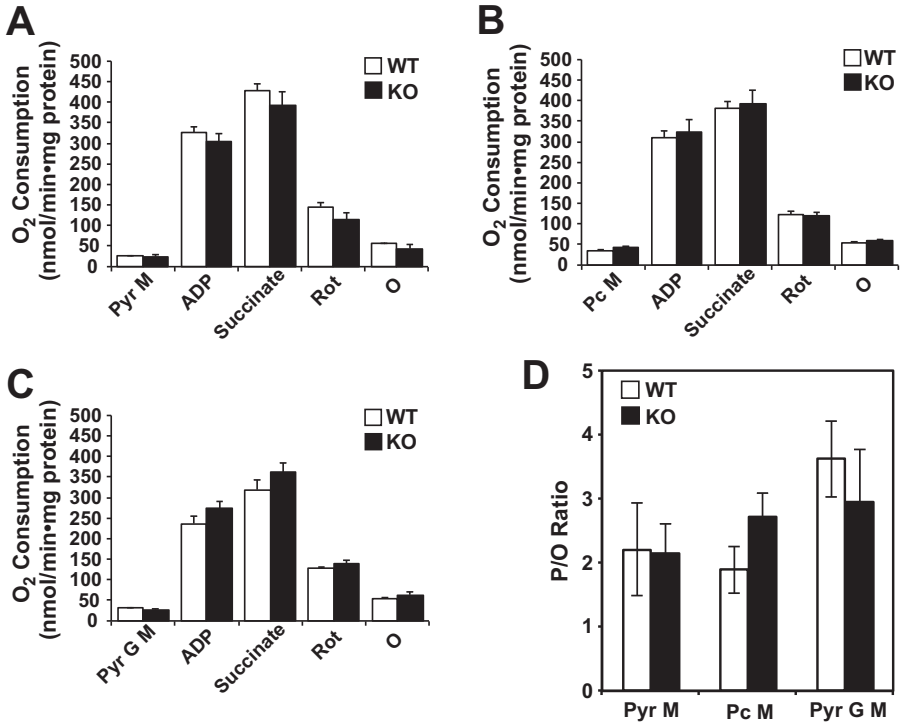

FIGURE 2. **High resolution respirometry of mitochondria from wild-type and cardiac myocyte-specific iPLA$_2\gamma$ knock-out mice.** Heart mitochondria isolated from wild-type Cre$^+$ (*WT*) and cardiac myocyte-specific iPLA$_2\gamma$ knock-out (*KO*) mice were utilized to measure oxygen consumption and ATP production in the presence of the indicated substrates as described under "Experimental Procedures." Oxygen consumption rates are expressed as nmol of O_2/min·mg of protein in the presence of: *A,* pyruvate and malate (*Pyr M*); *B,* palmitoylcarnitine and malate (*Pc M*); *C,* pyruvate, glutamate, and malate (*Pyr G M*). ADP (1.25 mM), succinate (5 mM), rotenone (*Rot*, 0.5 μM), and oligomycin (*O*, 2.5 μM) were sequentially added. *D,* ATP to oxygen (*P/O*) ratios for WT and CMiPLA$_2\gamma$KO (*KO*) mice were determined by measurement of ATP production and O_2 consumption during state 3 respiration in the presence of ADP for 3 min. Data are presented as means ± S.E. (n = 3–4/group) from male mice 6 months of age. No significant differences in mitochondrial respiration and P/O ratios were found in WT *versus* CMiPLA$_2\gamma$KO mouse myocardium as determined by Student's test.

Lipidomic Analyses of Myocardium from WT and CMiPLA$_2\gamma$KO Mice—To determine alterations in the myocardial lipidome of WT *versus* CMiPLA$_2\gamma$KO mice, we utilized multidimensional mass spectrometry-based shotgun lipidomics (MDMS-SL) (26). The major phospholipid classes in myocardium are choline and ethanolamine glycerophospholipids. Examination of choline glycerophospholipids demonstrated the presence of over 45 molecular species in murine myocardium that were largely composed of diacyl (D) phosphatidylcholine molecular species containing D16:0–22:6/D18:2–20:4, D18:0–22:6, D16:0–20:4/D18:2–18:2, D18:2–22:6, and D18:0–20:4/D18:2–20:2 in both the WT and the CMiPLA$_2\gamma$KO mice. Mirror plots of choline glycerophospholipids from averaged tandem mass spectra collected from six different mice demonstrated nearly identical profiles of individual molecular species (Fig. 3*A*). Similarly, MDMS-SL analysis of ethanolamine glycerophospholipids demonstrated over 30 diacyl phosphatidylethanolamine molecular species largely composed of D18:0–22:6, D16:0–22:6, D18:1–22:6, and D18:0–20:4 molecular species as well as 20 plasmenyl (P) ethanolamine phospholipid molecular species largely composed of P16:0–22:6, P18:1–20:4/P16:0–22:5, P18:0–22:6, and P18:1–22:6 molecular species. Mirror plots of ethanolamine glycerophospholipids from averaged mass spectra from six separate mice did not identify any significant differences between WT and CMiPLA$_2\gamma$KO mouse hearts (Fig. 3*B*). Triglyceride analysis by MDMS-SL demonstrated nearly identical total amounts of triglycerides and no differences in their molecular species composition in WT *versus* CMiPLA$_2\gamma$KO mice (Fig. 3*C*). Negative ion mass spectra did not reveal any significant differences in phosphatidylinositol, phosphatidylserine, or phosphatidylglycerol molecular species (Fig. 3*D*).

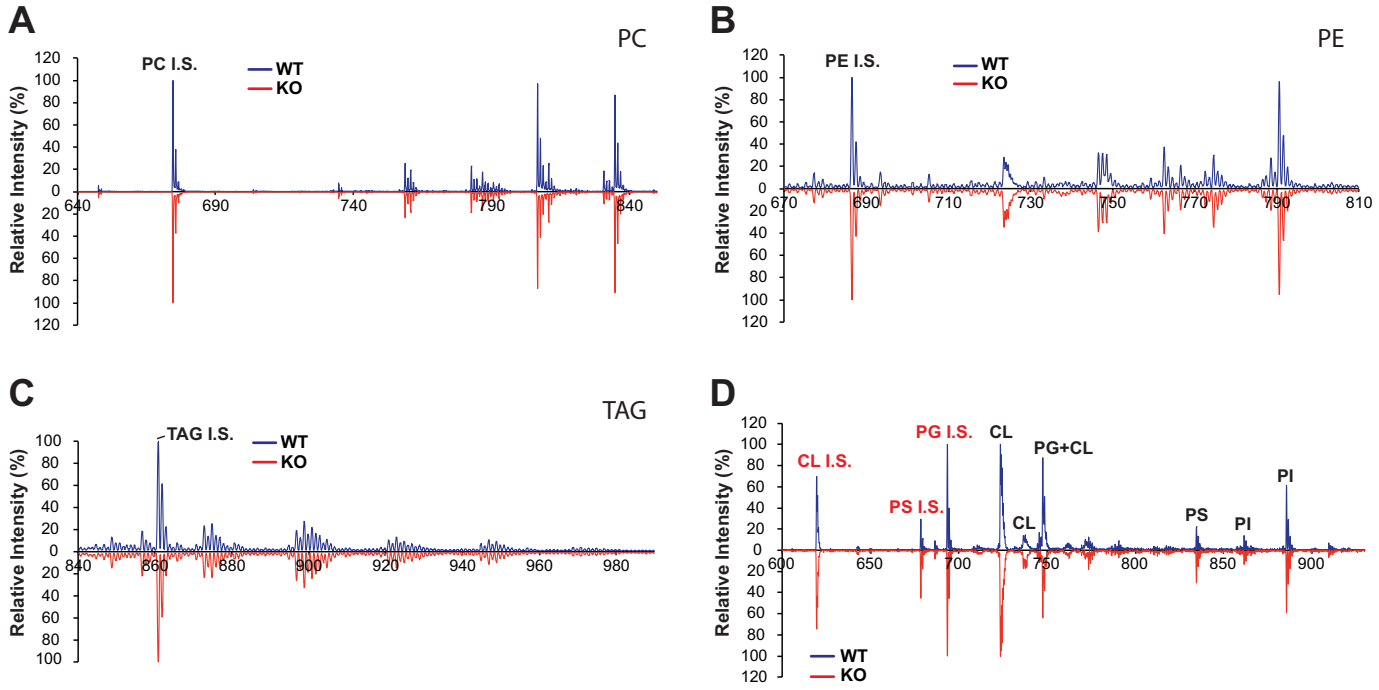

FIGURE 3. **Mass spectrometric analysis of choline phospholipids, ethanolamine phospholipids, triglycerides, and anionic phospholipids by molecular ion spectra or tandem MS/MS spectra of lipid extracts of wild-type (*WT*) and cardiac myocyte-specific iPLA$_2\gamma$ knock-out (*KO*) myocardium.** *A,* averaged mass spectra of precursor ion scanning of *m/z* 184.1 (at collision energy 35 eV) of choline phospholipid (*PC*) molecular species in the positive ion mode from WT and CMiPLA$_2\gamma$KO mouse myocardium. *B,* averaged molecular ion mass spectra of ethanolamine phospholipid (*PE*) molecular species in the negative ion mode from WT and CMiPLA$_2\gamma$KO mouse myocardium. *C,* averaged molecular ion mass spectra of ammoniated triglyceride molecular species in the positive ion mode from WT and CMiPLA$_2\gamma$KO mouse myocardium. *D,* averaged molecular ion mass spectra of negatively charged phospholipid molecular species in the negative ion mode from WT and CMiPLA$_2\gamma$KO mouse myocardium. *CL,* cardiolipin; *PG,* phosphatidylglycerol; *PI,* phosphatidylinositol; and *PS,* phosphatidylserine. All spectra were averaged from acquired individual mass spectra from four WT and six CMiPLA$_2\gamma$KO mice (~6–7 months of age) after normalization to the peak intensity of internal standard (I.S.) in each panel (*i.e.* phosphatidylcholine I.S. in *A*; phosphatidylethanolamine I.S. in *B*; triacylglycerol I.S. in *C*; and PG I.S. in *D*).

Next, because tetra-18:2 cardiolipin (CL) has been previously proposed to enhance mitochondrial efficiency by stabilizing the formation of mitochondrial supercomplexes (27–30), we determined the content and composition of myocardial CL using the M+1/2 isotopologue approach (Fig. 4) (31). The results demonstrated no significant differences in the total content of CL. The composition of most molecular species of CL, including symmetric tetra-18:2 CL (*m/z* 723.5 in Fig. 4*A*) in WT *versus* CMiPLA$_2\gamma$KO myocardium, were nearly identical. Modest decreases in the levels of 18:2–18:2–18:2–22:6 CL and 18:2–18:2–22:6–22:6 CL (*m/z* 747.5 and *m/z* 771.5, respectively, in Fig. 4*A*) were present in CMiPLA$_2\gamma$KO mice (Fig. 4*B*).

Mass Spectrometric Analysis of Myocardial Eicosanoids, Docosanoids, and Oxidized Linoleic Acids—Previous studies have demonstrated the important roles of iPLA$_2\gamma$ in releasing polyunsaturated fatty acids from mitochondria that are subsequently oxidized by a wide variety of downstream oxygenases (32–35). To gain access to the extremely low abundance regime necessary for accurate identification and quantification of oxidized fatty acids in myocardium, we used charge-switch derivatization with multiple reaction monitoring (MRM) in conjunction with high mass accuracy analysis of signature product ions from diagnostic transitions (36). Multiple differences in oxidized fatty acids containing 18-, 20-, and 22-carbons were observed in CMiPLA$_2\gamma$KO mice (Fig. 5). These include decreases in prostaglandins, 11-hydroxy-5*Z*,8*Z*,12*E*,14*Z*-eicosatetraenoic acid (11-HETE), 12-hydroxy-5*Z*,8*Z*,10*E*,14*Z*-eicosatetraenoic acid (12-HETE), and 15-hydroxy-5*Z*,8*Z*,11*Z*,13*E*-eicosatetraenoic acid (15-HETE) as well as increased levels of 14(15)-epoxy-5*Z*,8*Z*,11*Z*-eicosatrienoic acid (14,15-EET). Similarly, CMiPLA$_2\gamma$KO mice had decreased levels of all observable oxidized linoleic acid metabolites (oxlams) except 9-oxo-10*E*,12*Z*-octadecadienoic acid (9-oxoODE) and had significant decreases in 22-carbon oxidized fatty acids, including 7*S*,8*R*,17*S*-trihydroxy-4*Z*,9*E*,11*E*,13*Z*,15*E*,19*Z*-docosahexaenoic acid (RVD-1), 19,20-dihydroxy-4*Z*,7*Z*,10*Z*,13*Z*,16*Z*-docosapentaenoic acid, and 7-hydroxy-4*Z*,8*E*,10*Z*,13*Z*,16*Z*,19*Z*-docosahexaenoic acid (7-HDoHE) (Fig. 5). These results identify iPLA$_2\gamma$ as a prominent enzymic mediator for the generation of signaling oxidized fatty acids in myocardium.

Decreased Susceptibility of mPTP Opening in Myocardium from CMiPLA$_2\gamma$KO Mice in Comparison with Wild-type Mice—Recent work in our laboratory led to the identification of iPLA$_2\gamma$ as an important modulator of the Ca^{2+}-induced opening of the mPTP in mitochondria isolated from liver (9). To determine the contribution of iPLA$_2\gamma$ to the opening of the cardiac myocyte mPTP, we compared Ca^{2+}-induced mitochondrial swelling in WT *versus* CMiPLA$_2\gamma$KO mice. Incubation with calcium resulted in the anticipated swelling of WT myocardial mitochondria due to opening of the mPTP. In marked contrast, mitochondrial swelling was substantially attenuated in CMiPLA$_2\gamma$KO mice (Fig. 6). Ca^{2+}-induced swelling of mitochondria from both WT and CMiPLA$_2\gamma$KO mice was demonstrated to be cyclophilin D (also known as peptidyl-prolyl cis-trans isomerase F)-dependent through nearly complete inhibition by 2 μM cyclosporin A. No observable differ-

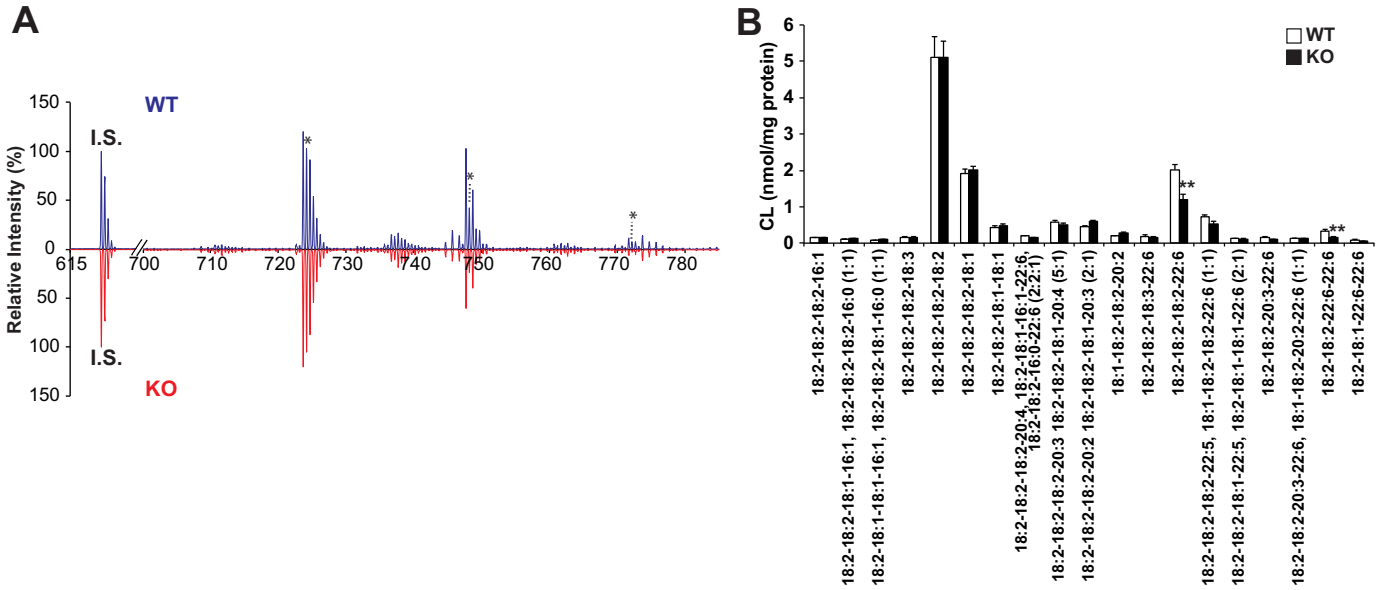

FIGURE 4. **Mass spectrometric analysis of cardiolipin molecular species in wild-type and cardiac myocyte-specific iPLA$_2\gamma$ KO myocardium.** *A,* representative negative ion mode mass spectrum of anionic lipids for myocardium cardiolipin (*CL*) analysis from wild-type (*WT*) and cardiac myocyte-specific iPLA$_2\gamma$ KO (*KO*) mice (6–7 months of age) after normalizing to tetra-14:0 CL internal standard (I.S., *m/z* 619.5). Cardiolipin molecular species were identified by the doubly charged peaks. The *asterisks* indicate examples of the M + 1/2 isotopologues of the doubly charged cardiolipin species (*e.g.* tetra-18:2 CL; 18:2–18:2–18:2–22:6 CL; and 18:2–18:2–22:6–22:6 CL) whose ion peak intensities were utilized to quantify individual cardiolipin molecular species. Tetra-18:2 CL is the predominant cardiolipin molecular species present at *m/z* 723.5. *B,* cardiolipin molecular species were identified in WT ($n = 4$) and CMiPLA$_2\gamma$KO (*KO*) mouse myocardium ($n = 6$). **, $p < 0.01$.

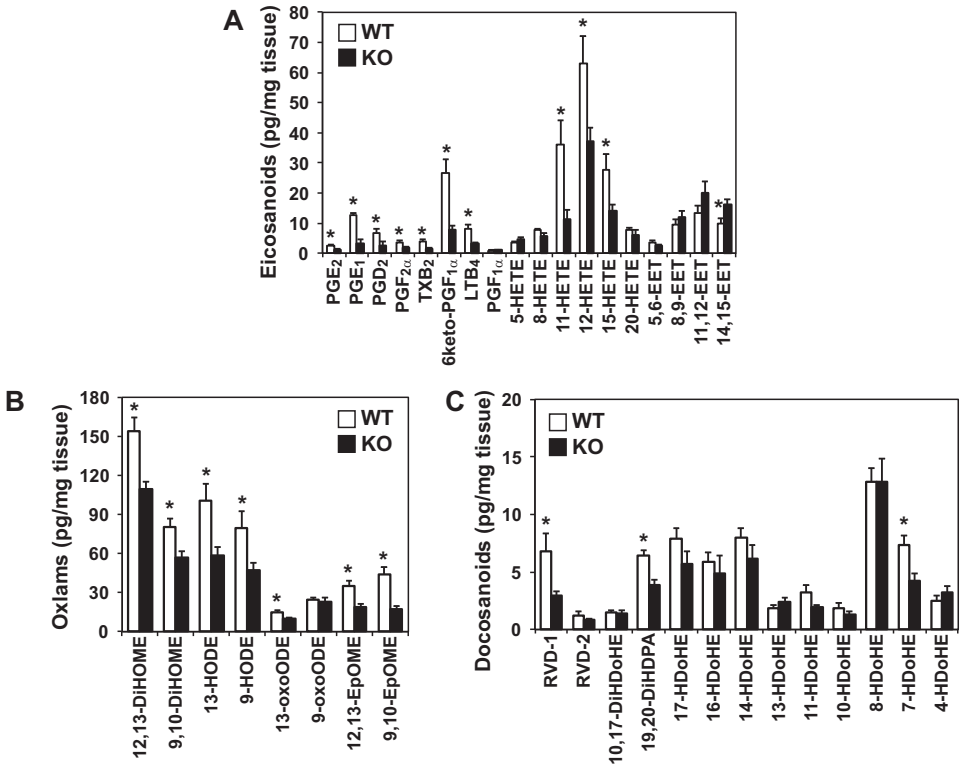

FIGURE 5. **Cardiac oxidized fatty acids in wild-type and cardiac myocyte-specific iPLA$_2\gamma$ KO myocardial tissue.** Myocardial tissue was isolated from wild-type (*WT*) and CMiPLA$_2\gamma$KO (*KO*) mice (~6–7 months of age) and flash-frozen in liquid nitrogen. Eicosanoids (*A*), oxlams (*B*), and docosanoids (*C*) were then purified by solid phase extraction and derivatized with AMPP. Quantitative analysis was performed by LC-MS/MS via MRM in the positive ion mode with accurate mass analysis of diagnostic product ions following separation of molecular species using a reverse phase column as described under "Experimental Procedures." Values are the means ± S.E. of six preparations. *, $p < 0.05$ when compared with KO. *HETE,* hydroxyeicosatetraenoic acid; *EET,* epoxyeicosatrienoic acid; *DiHOME,* dihydroxyoctadecenoic acid; *HODE,* hydroxyoctadecadienoic acid; *oxoODE,* oxo-octadecadienoic acid; *EpOME,* epoxyoctadecenoic acid; *LTB$_4$,* leukotriene B$_4$; *TXB,* thromboxane B; *PG,* prostaglandin; *RVD,* resolvin; *DiHDoHE,* dihydroxydocosahexaenoic acid; *DiHDPA,* dihydroxydocosapentaenoic acid; and *HDoHE,* hydroxydocosahexaenoic acid.

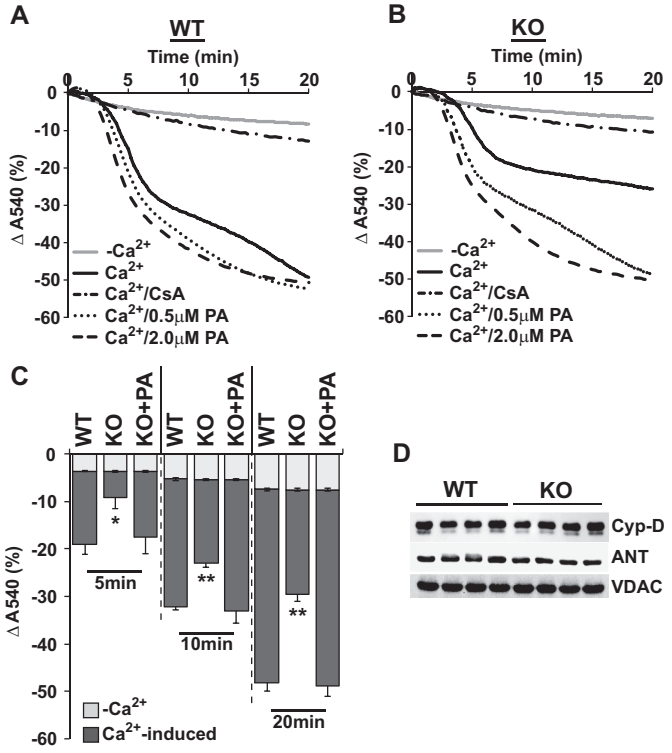

FIGURE 6. **Kinetics of calcium-induced swelling of mitochondria from wild-type and cardiac myocyte-specific iPLA$_2$γ knock-out mice.** Myocardial mitochondria were isolated by differential centrifugation from wild-type (*WT*) and CMiPLA$_2$γKO (*KO*) mice (6 months old) and resuspended in swelling buffer containing 0.23 M mannitol, 70 mM sucrose, 2 mM KH_2PO_4, 3 mM HEPES, pH 7.0, 5 mM succinate, and 1.25 μM rotenone. Mitochondria were placed in a 96-well plate with ethanol vehicle alone (1%), 2 μM cyclosporin A (*CsA*), 0.5 or 2 μM palmitate (*PA*). Following exposure to either 150 μM Ca^{2+} or 10 μM EGTA ($-Ca^{2+}$), WT (*A*) and KO (*B*) mitochondrial swelling was monitored for decreases in absorbance at 540 nm at 15-s intervals at 23 °C. Net changes in absorbance at 540 nm at 5, 10, and 20 min in WT and KO mitochondria were calculated in *C* where *, $p < 0.05$ and **, $p < 0.001$ when compared with the Ca^{2+}-induced absorbance decrease in WT mitochondria. Values are the average of four independent preparations ± S.E. Western blots against cyclophilin D (*Cyp-D*), adenine nucleotide translocase (*ANT*), and voltage-dependent anion channel (*VDAC*) in WT and CMiPLA$_2$γKO (*KO*) mouse hearts are shown in *D* ($n = 4$).

ences in cyclophilin D and adenine nucleotide translocase protein expression levels were present in WT *versus* CMiPLA$_2$γKO myocardium indicating that the attenuation of mPTP opening in CMiPLA$_2$γKO mice is not due to alterations in the expression of regulatory machinery of the mPTP by ablation of iPLA$_2$γ (Fig. 6*D*). Because iPLA$_2$γ selectively releases palmitate from the *sn*-1 position of polyunsaturated phospholipids, we investigated the role of low concentrations of palmitate on mPTP opening in WT and CMiPLA$_2$γKO mice. Addition of as little as 500 nM palmitate to mitochondria isolated from CMiPLA$_2$γKO mice completely recapitulated the calcium-induced swelling present in WT mice (Fig. 6).

Ischemia/Reperfusion Results in Dramatic Increases in Signaling Oxidized Fatty Acids That Are Attenuated in the CMiPLA$_2$γKO Mouse—Next, we determined whether iPLA$_2$γ loss of function results in alterations in lipid second messenger production during 30 min of ischemia followed by 30 min of reperfusion *in vivo*. High mass accuracy mass spectrometric analysis demonstrated 10–30-fold increases in multiple oxidized 18-, 20-, and 22-carbon fatty acids (*i.e.* oxlams, eicosanoids, and docosanoids, respectively) in the ischemic border zone *versus* non-ischemic regions of WT control hearts following I/R (Fig. 7). This dramatic increase was markedly attenuated in the border zone of ischemia in CMiPLA$_2$γKO mouse hearts. We specifically point out that the majority of signaling fatty acids induced by I/R result from lipoxygenase, cytochrome P450, and/or other oxidases acting on polyunsaturated fatty acids and do not originate from cyclooxygenase-mediated oxidation. These results are suggestive of fatty acid metabolic channeling from iPLA$_2$γ to downstream lipoxygenase, P450, and/or other as yet unidentified mitochondrial fatty acid oxidases.

Oxidized Fatty Acids, Including HETEs and 8-HDoHE, Facilitate Ca^{2+}-mediated Mitochondrial Membrane Depolarization—Because severe mitochondrial membrane depolarization is manifest upon calcium challenge, we investigated the effects of the oxidized fatty acid metabolites that dramatically increase during I/R on Ca^{2+}-mediated membrane depolarization of myocardial mitochondria. Mitochondrial membrane potential ($\Delta\Psi_{mt}$) was determined by using a tetraphenylphosphonium (TPP^+) ion-selective electrode as described under "Experimental Procedures." By measuring the extramitochondrial concentration of TPP^+, the changes in mitochondrial membrane potential were monitored following Ca^{2+} titration in the presence of either vehicle (ethanol), 12-HETE, 20-HETE, 14,15-EET, PGE_2, 9-oxoODE, or 8-HDoHE, all of which were dramatically increased during I/R *in vivo* (see Fig. 7). The initial $\Delta\Psi_{mt}$ (approximately −160 mV) became less negative rapidly upon sequential calcium additions in the presence of either vehicle alone (control), 14,15-EET, PGE_2, or 9-oxoODE, but the membrane potential was partially restored within 4 min (Fig. 8). In contrast, 12-HETE, 20-HETE, or 8-HDoHE greatly facilitated mitochondrial depolarization at 60–80 μM calcium ion by dissipating the electric potential across the membrane resulting in no further depolarization upon addition of an uncoupling agent, trifluoromethoxy carbonylcyanide phenylhydrazone (FCCP) (Fig. 8).

Cardiac Myocyte-specific Ablation of iPLA$_2$γ Results in Dramatic Protection from Myocardial Ischemia/Reperfusion Injury in Vivo—Because mitochondria from CMiPLA$_2$γKO myocardium are resistant to mPTP opening and contained decreased amounts of inflammatory oxidized fatty acids that promote Ca^{2+}-mediated mitochondrial depolarization, we hypothesized that the CMiPLA$_2$γKO heart would be protected from I/R injury. Accordingly, we induced myocardial ischemia *in vivo* by ligation of the left anterior descending coronary artery for 30 min followed by 24 h of closed chest reperfusion, and we compared the infarct area to the area-at-risk in WT *versus* CMiPLA$_2$γKO mice. In WT mice, ischemia/reperfusion resulted in infarction of 40% of the area-at-risk (Fig. 9). Remarkably, in CMiPLA$_2$γKO mice, iPLA$_2$γ loss of function protected the heart from ischemia/reperfusion damage resulting in reduction of the infarct area to 16% of the area-at-risk (Fig. 9). Taken together, these results demonstrate that iPLA$_2$γ plays a prominent role in I/R-induced cardiac myocyte cell death illuminating iPLA$_2$γ inhibition as a novel multitiered therapeutic approach to significantly reduce infarct size during I/R.

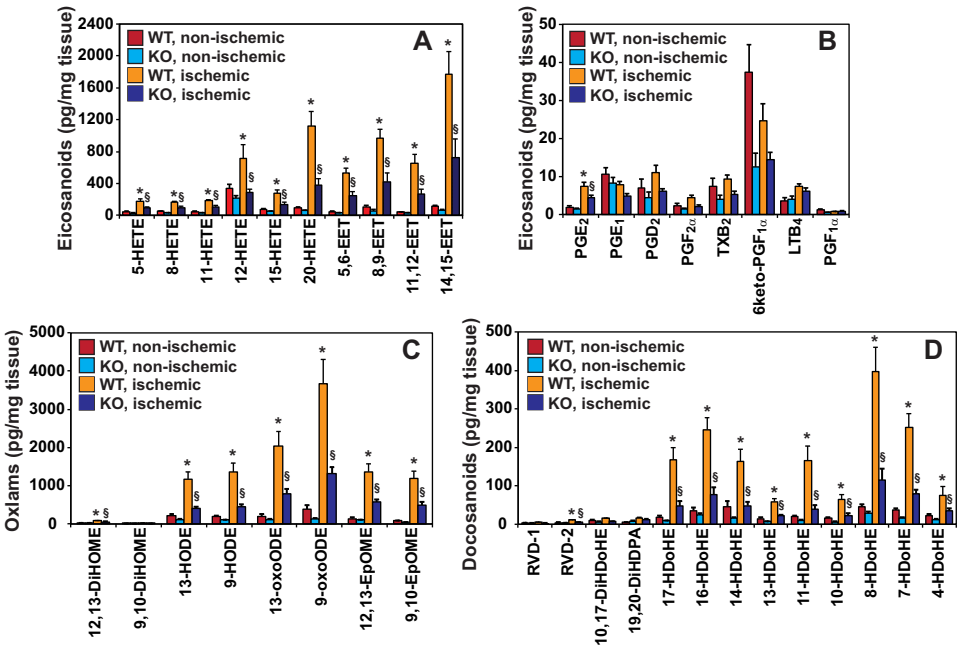

FIGURE 7. **Oxidized metabolites of arachidonic acid, linoleic acid, and docosahexaenoic acid in non-ischemic and ischemic border zones of myocardium from wild-type and cardiac myocyte-specific iPLA$_2$γ knock-out mice following ischemia/reperfusion.** Oxidized fatty acid metabolites from non-ischemic and ischemic myocardial zones of wild-type (*WT*) and CMiPLA$_2$γKO (*KO*) mice were extracted, isolated by solid phase extraction, derivatized with AMPP, and quantitated by LC MS/MS via MRM in the positive ion mode with accurate mass analysis of diagnostic product ions following separation of molecular species using a reverse phase C18 column. Significant decreases in the production of multiple identified oxidized metabolites of arachidonic acid (*A* and *B*), linoleic acid (*C*), and docosahexaenoic acid (*D*) in ischemic border zones are present as a result of cardiac myocyte-specific ablation of iPLA$_2$γ. Significant increases in the production of multiple identified oxidized metabolites in ischemic border zones compared with non-ischemic zones were also demonstrated. Values presented are the means ± S.E. Comparisons were made using Student's *t* test ($n = 6$). *, $p < 0.05$ *versus* WT non-ischemic. §, $p < 0.05$ when compared with WT, ischemic. Refer to Fig. 5 legend for oxylipin abbreviations.

Discussion

Previous studies have emphasized the central roles of the mPTP in mediating cardiac damage during ischemia/reperfusion through opening of the channel precipitated by calcium overload, accumulation of inorganic phosphate, and induction of oxidative stress that is amplified by the production of saturated fatty acids and oxidized lipid metabolites (4, 37, 38). The large amounts of acyl-CoA and acylcarnitine that accumulate in the mitochondrial matrix during ischemia accelerate mPTP opening and are directly released into the cytosol along with cytochrome *c* after mPTP opening (9, 39, 40). Prolonged Ca^{2+}-induced opening of the mPTP that is facilitated by Ca^{2+} activation of iPLA$_2$γ causes irreversible dissipation of the mitochondrial membrane potential and loss of membrane integrity leading to extensive mitochondrial damage (41). The resultant mitochondrial depolarization exacerbates mitochondrial dysfunction by autoamplification of membrane potential-sensitive iPLA$_2$γ activity (42). Furthermore, mPTP opening results in the release of apoptogenic factors (*e.g.* cytochrome *c* and apoptosis-inducing factor) from the intermembrane space that triggers cell death programs rather than homeostatic clearance of metabolically inefficient mitochondria (*e.g.* mitophagy). This study demonstrates the unanticipated and dramatic accumulation of oxidized fatty acids, including large amounts of oxidized linoleic acid metabolites, which likely originate from cardiolipin, the major pool of esterified linoleic acid in the mitochondrial compartment as well as a plethora of eicosanoid metabolites known to have adverse effects on cardiac myocyte membrane proteins, inflammation, and bioenergetics (43–45). The benefits of iPLA$_2$γ loss of function investigated in this study include the attenuation of many of the molecular mechanisms known to predispose to myocardial tissue damage during pathological processes, including cardiac ischemia/reperfusion (46).

Consistent with our prior work identifying iPLA$_2$γ as an important regulator of the calcium-induced opening of the mPTP in liver mitochondria (9), myocardial mitochondria from the CMiPLA$_2$γKO mouse demonstrate the regulatory role of cardiac iPLA$_2$γ on the mitochondrial permeability transition. Furthermore, we demonstrated that submicromolar concentrations of free palmitic acid restored mPTP opening that was attenuated by loss of myocardial iPLA$_2$γ. This is particularly relevant because iPLA$_2$γ has a marked *sn*-1 regiospecificity for hydrolysis of diacyl phospholipids containing *sn*-2 arachidonic acid or docosahexaenoic acid leading to the release of saturated fatty acids from the *sn*-1 position concomitant with the generation of 2-arachidonoyl- and 2-docosahexaenoyl-lysolipids, respectively, in the mitochondrial membrane (25). The rapid lateral diffusion of the released saturated fatty acid in the plane of the inner membrane allows it to directly interact with the mPTP without sequestration by cytosolic fatty acid-binding proteins. The regulatory effects of palmitate on the mPTP are further aggravated by its ability to induce ER Ca^{2+} depletion and reactive oxygen species generation (47, 48) and by acting as an endogenous ionophore (49). Supporting these mechanisms, deletion of mitochondrial membrane-associated iPLA$_2$γ led to the remarkable and robust salvage of damaged regions of myocardium after I/R, which emphasizes a prominent role of car-

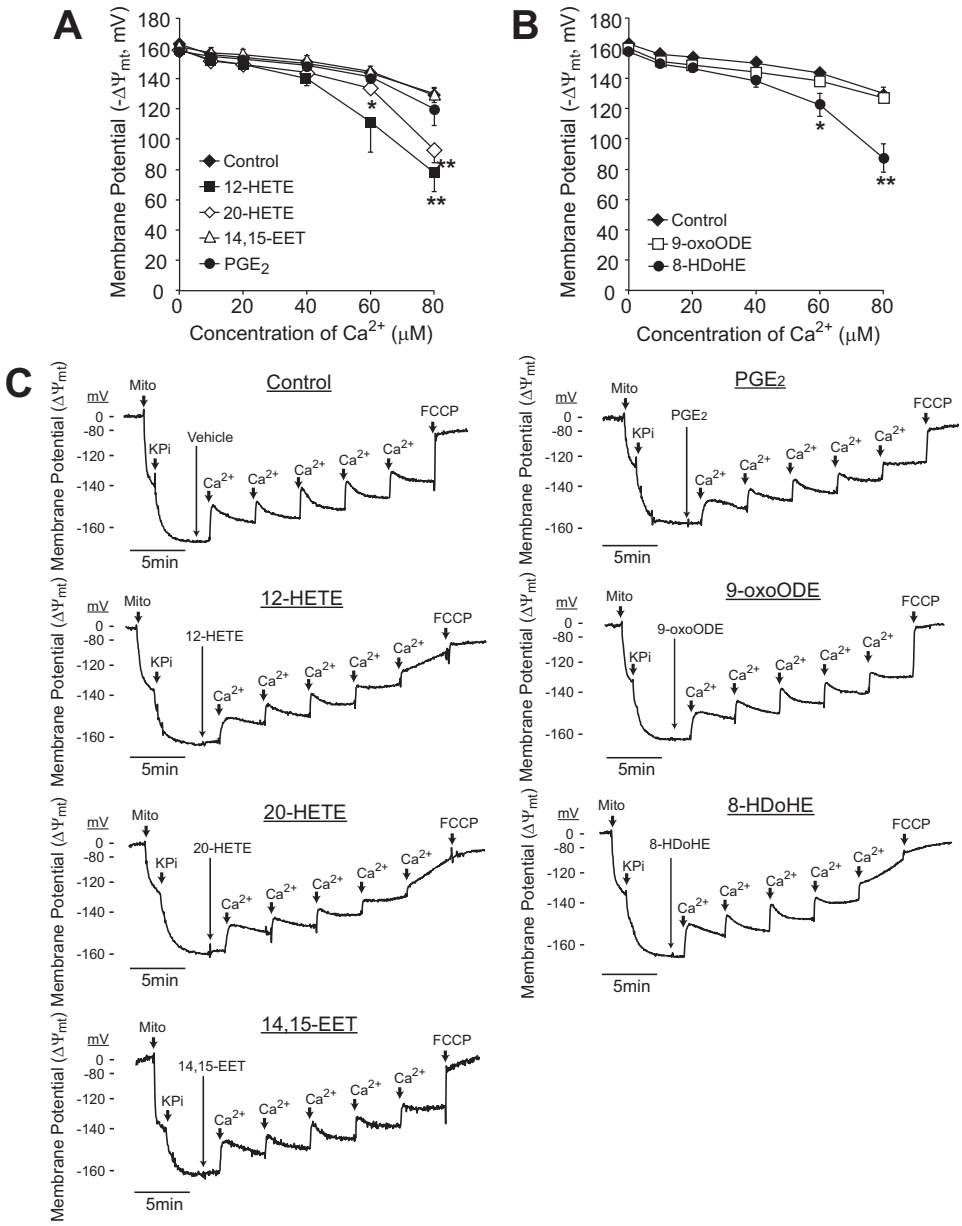

FIGURE 8. **Facilitation of Ca^{2+}-mediated mitochondrial membrane depolarization by oxidized polyunsaturated fatty acids.** *A* and *B,* mitochondria were isolated from C57BL/6J mice (4–5 months of age) and 0.125 mg of protein/ml of mitochondria (*mito*) were placed into an OROBOROS Oxygraph 2K chamber containing a buffer solution of 0.23 M mannitol, 0.07 M sucrose, 3 mM HEPES, pH 7.4, 5 mM succinate, and 2 μM tetraphenylphosphonium chloride (TPP·Cl). The final concentrations of 0.1 mM KH_2PO_4 (KP_i) and 1 μM oxidized fatty acids, including 12-HETE, 20-HETE, 14,15-EET, PGE_2, 9-oxoODE, and 8-HDoHE, or ethanol vehicle (control) were added to the chamber at the indicated times (*arrows*). $CaCl_2$ was sequentially added at 4-min intervals to the final concentrations of 10, 20, 40, 60, and 80 μM. Mitochondrial membrane potential ($\Delta\Psi_{mt}$) was determined by the concentration of extramitochondrial TPP^+ measured with an ion-selective electrode. Maximum depolarization of mitochondria was observed in the presence of 1.5 μM FCCP. *, $p < 0.05$, and **, $p < 0.01$ by Student's test when compared with the controls ($n = 3–4$). *C,* representative potentiometric tracings are shown.

diac myocyte iPLA$_2$γ in facilitating mPTP opening and the resultant increase in infarct size.

In addition to iPLA$_2$γ-mediated release of saturated fatty acids from phospholipid pools, we previously reported marked iPLA$_2$γ-dependent production of cardiac eicosanoids in the myocardium by utilizing cardiac myocyte-specific overexpression of iPLA$_2$γ and global iPLA$_2$γ knock-out mice (34). Our previous findings suggest that iPLA$_2$γ-generated 2-polyunsaturated fatty acyl lysolipids and their downstream hydrolytic products (non-esterified polyunsaturated fatty acids) are further channeled to multiple metabolic pathways to produce numerous oxidative metabolites (34, 50). A variety of oxidized polyunsaturated lipids generated by multiple oxygenases (*e.g.* cyclooxygenases, lipoxygenases, and P450 hydroxylases) have been identified as pro-inflammatory mediators in diverse tissues and cell types (45, 51). The deleterious sequelae of pro-inflammatory oxylipins in myocardial I/R injury are also well known, although the precise complement and functions of individual signaling oxylipin molecular species are poorly understood (52–54). To determine the types and changes in extremely low abundance signaling oxidized fatty acids released during pathological processes, we utilized a mass spectrometric "charge-switch" high mass accuracy product ion approach that resulted in a marked increase in sensitivity and

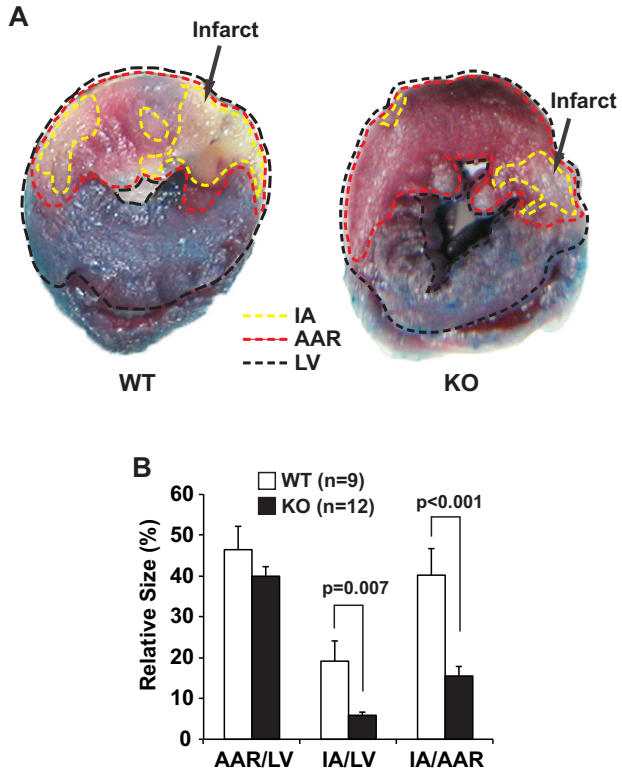

FIGURE 9. **Cardiac myocyte-specific ablation of iPLA$_2\gamma$ decreases infarct size in ischemic zones following ischemia/reperfusion.** *A,* stained ventricular slices of hearts from either WT or CMiPLA$_2\gamma$KO (*KO*) mouse hearts at similar levels demonstrate excellent definition of the areas of infarction (*IA* bordered by *yellow dashed line*, *arrows*), area-at-risk (*AAR*, *red dashed line*), and the left ventricle (*LV*, *black dashed line*) after a 30-min occlusion and 24 h of reperfusion of the left anterior descending artery (*LAD*). At the end of the reperfusion interval, the heart was excised and perfused with Phthalo blue dye with the LAD reoccluded (to define the previous area-at-risk) followed by TTC staining to define the infarct size. *B,* dramatic decreases in IA/left ventricle and IA/area-at-risk were quantified and subjected to statistical analysis. Data are presented as means ± S.E. utilizing 9 WT and 12 KO male mice (~6–7 months of age).

successful exclusion of false-positive identification through high mass accuracy analysis of informative product ions (36). Although the myocardial lipidome of CMiPLA$_2\gamma$KO mice is relatively unaltered in comparison with WT, the decrease in numerous low abundance oxidized free fatty acids was evident in CMiPLA$_2\gamma$KO mouse myocardium under basal conditions. The presence of large amounts of oxlams in WT murine myocardium was unanticipated and suggests their previously unknown roles in myocardial signaling. The observation that oxlams were so prominent suggests that their oxidation occurred predominantly in the mitochondrial compartment that is rich in 18:2 fatty acids esterified to cardiolipin. Moreover, the finding of dramatic increases in multiple oxidized lipid second messengers present in the infarct border zone after I/R, which were substantially reduced in the CMiPLA$_2\gamma$KO mouse, identifies iPLA$_2\gamma$ as the rate-determining step for the pathological production of these oxylipins during I/R injury.

Because oxidized fatty acids have a multitude of effects on transmembrane proteins, including ion channels and receptors (55, 56), we monitored the changes in mitochondrial membrane potential ($\Delta\Psi_{mt}$) in the presence of multiple oxidized lipid metabolites to determine their effects on Ca^{2+}-mediated potential dissipation. During sequential calcium challenges, mitochondria in the absence of extramitochondrial oxidized fatty acids partially recovered their membrane potential from multiple rapid initial losses of transmembrane potential induced by additions of Ca^{2+}. In contrast, hydroxylated polyunsaturated fatty acids (*e.g.* 12-HETE, 20-HETE, and 8-HDoHE), but not 14,15-EET, 9-oxoODE, or PGE_2, sensitize mitochondria to the calcium-induced loss of membrane potential. These findings are supported by previous studies that showed arachidonic acid- and 12-HETE-facilitated Ca^{2+} overload resulting in abnormal oxidative stress and mitochondrial dysfunction (44, 49). Therefore, the results of this study suggest that iPLA$_2\gamma$ facilitates production of oxidized lipid metabolites by providing PUFAs and/or polyunsaturated fatty acyl lysolipids, which can be further hydrolyzed to non-esterified PUFAs by lysophospholipases and subsequent oxidation by downstream oxygenases. The resultant oxidized fatty acids likely regulate ion channels through selective binding to transmembrane domains of ion channels and ion transporters, direct disruption of interactive membrane domains, and/or the formation of pores in the membrane bilayer. Collectively, it seems likely that the enzymic activity of iPLA$_2\gamma$ integrates metabolic information from multiple pathways to regulate myocardial networks that control cell fate decisions, electrophysiological function, and receptor-mediated alterations in cardiac myocyte metabolism.

Taken together, this study identifies a critical role of cardiac myocyte iPLA$_2\gamma$ in the Ca^{2+}-induced opening of the mPTP and the generation of inflammatory signaling oxidized fatty acids that each contribute to cardiac damage during I/R, which can be largely ablated by iPLA$_2\gamma$ loss of function. Thus, inhibition of a single enzyme has multiple salutary effects during I/R providing a novel synergistic approach for the pharmacological treatment of acute coronary syndromes and multiple myocardial diseases.

Experimental Procedures

Materials—PCR reagents were purchased from Applied Biosystems (Foster City, CA) for genotyping of WT and CMiPLA$_2\gamma$KO mice. Radiolabeled nucleotides ([α-^{32}P]dCTP) were purchased from PerkinElmer Life Sciences. Synthetic phospholipids used as internal standards in mass spectrometric analyses were purchased from either Avanti Polar Lipids (Alabaster, AL) or Nu-Chek Prep, Inc. (Elysian, MN). Oxylipins, including deuterated stable isotopes used as internal standards, and FCCP were obtained from Cayman Chemical (Ann Arbor, MI). Tamoxifen utilized for heart-specific conditional ablation of iPLA$_2\gamma$ was obtained from Sigma. Anti-iPLA$_2\gamma$ antibody was generated in our laboratory as described previously (9). Cyclosporin A was obtained from EMD Millipore (Billerica, MA). Antibodies for cyclophilin D, voltage-dependent anion channel, and adenine nucleotide translocase were purchased from Santa Cruz Biotechnology, Inc. (Dallas, TX). Most other supplies and reagents were obtained from Sigma or Fisher.

General Animal Studies—Animal protocols were in strict accordance with guidelines of the National Institutes of Health Office of Laboratory Animal Welfare and were approved by the Animal Studies Committee at Washington University. Mice

were fed a standard diet (PicoLab Rodent 20 from LabDiet (St. Louis, MO) containing 5% total fat (13% of total calories) and 0.94% saturated fat) *ad libitum* unless otherwise indicated. Echocardiographic analyses were performed under light anesthesia as described previously (57, 58). Following euthanasia by cervical dislocation, heart tissues were dissected from male mice, weighed, and either flash-frozen in liquid N_2 or the fresh tissue was used immediately.

Generation of Cardiac Myocyte-specific iPLA$_2\gamma$ Knock-out Mice—To elucidate the specific roles of iPLA$_2\gamma$ in myocardium, we engineered a conditional iPLA$_2\gamma$ targeting construct containing 7208 bases of the mouse iPLA$_2\gamma$ gene (mouse BAC clone bMQ-391E22, Geneservice Ltd., Cambridge, UK) with an inserted loxP-flippase (FLP) recombinase target (FRT)-neomycin-FRT resistance cassette and a loxP site encompassing exon 5 of the iPLA$_2\gamma$ gene (Fig. 1). Deletion of exon 5 has been previously shown to result in a genotype null for iPLA$_2\gamma$ and complete ablation of iPLA$_2\gamma$ protein expression in multiple tissues (22). The sequence of the targeting vector was verified prior to electroporation into EDJ22 ES cells at the Mouse Genetic Core, Washington University. PCR analyses using iPLA$_2\gamma$-specific primers 5′-TATAGAGATGCACAACCAGTGAAGCGCG-3′ and 5′-AGTTGGTAGTGTATGACTAGCACT-3′ identified three targeted ES clones; however, Southern blot analyses revealed that two of the clones also contained an additional random incorporation event. Therefore, only the ES cell clone containing the single targeted event was expanded and used for injection of blastocysts and implantation into pseudo pregnant female C57BL/6 mice. Chimeric mice were identified by PCR analyses of tail gDNA as described for the ES cell clones. F1 mice obtained from mating to C57BL/6 mice were similarly genotyped and revealed germ line transmission of the floxed target allele. Next, the PGK-neo cassette was removed by crossing with an FLP recombinase expressing mouse (stock no. 3800; The Jackson Laboratory). Deletion of the PGK-neo cassette by this FRT recombinase transgenic line was confirmed by PCR (Fig. 1*C*).

Our floxed iPLA$_2\gamma$ allele (abbreviated g^f/g^f) mice were next crossed with an αMHC-MerCreMer mouse line (stock no. 005657, The Jackson Laboratory), which produces a tamoxifen-inducible Cre recombinase in myocardium. The progeny were genotyped by duplex PCR using the above-mentioned iPLA$_2\gamma$-specific primers combined with Cre-specific primers 5′-CGGTCGATGCAACGAGTGATGAG-3′ and 5′-ACGAACCTGGTCGAAATCAGTGCG-3′ (Fig. 1). Transgenic αMHC-MerCreMer and g^f/g^f mice were backcrossed onto a C57BL/6 background for at least four generations prior to generating double transgenic αMHC-MerCreMer:g^f/g^f mice. Myocardial iPLA$_2\gamma$ gene ablation was induced in 1.5–3-month-old αMHC-MerCreMer:g^f/g^f mice by intraperitoneal tamoxifen injections (30 μg/gm body weight) twice daily for 2 consecutive days. Initially, two control groups of 3-month-old mice (one group possessing only the functional floxed iPLA$_2\gamma$ alleles (g^f/g^f) and a second group bearing the inducible Cre transgene but no loxP sites) were identically treated with tamoxifen. This dosage of tamoxifen in 3-month-old mice induced a level of Cre-recombinase that produces no observable pathology in controls but was sufficient to attain a null iPLA$_2\gamma$ gene.

Mass Spectrometric Analyses of Eicosanoids, Docosanoids, and Oxidized Metabolites of Linoleic Acid—Mass spectrometric analyses of signaling eicosanoids, docosanoids, and oxlams were performed using a charge-switch strategy by derivatization with *N*-(4-aminomethylphenyl) pyridinium (AMPP) and subsequent LC-MS/MS with MRM and accurate mass determination of diagnostic product ions as described previously (36).

MDMS-SL Analyses—Lipidomic analyses of WT and CMiPLA$_2\gamma$KO mouse myocardium were performed as described previously (22, 23). Lipid extracts were reconstituted with 1:1 (v/v) $CHCl_3/CH_3OH$, flushed with nitrogen and stored at −20 °C prior to electrospray ionization-MS using a TSQ Quantum Ultra Plus triple-quadrupole mass spectrometer (Thermo Fisher Scientific, San Jose, CA) equipped with an automated nanospray apparatus (Advion Biosciences Ltd., Ithaca, NY) and customized sequence subroutine operated under Xcalibur software. Enhanced MDMS-SL analysis of cardiolipins was performed with a mass resolution setting of 0.3 Thomson using the M +1/2 isotopologue approach as we described previously (31, 59).

Isolation of Mitochondria—Mice were euthanized by cervical dislocation, and their hearts were removed and placed in ice-cold mitochondria isolation buffer (MIB: 0.21 M mannitol, 0.07 M sucrose, 0.1 mM K-EDTA, 10 mM Tris-HCl, 1 mM EGTA, 0.5% BSA, pH 7.4) in a Petri dish on ice. Heart tissue was immediately diced into small pieces with a razor blade and transferred to a 10-ml Potter-Elvehjem tissue grinder with 5 ml of MIB. The tissue was homogenized using a rotorized homogenizer with a Teflon pestle set at 120 rpm. The homogenate was then diluted to 10 ml with MIB and centrifuged for 7 min at 850 × *g*. The supernatant was carefully collected and centrifuged at 10,000 × *g* for 10 min. The final pellet was resuspended in MIB with no BSA.

High Resolution Mitochondrial Respirometry—High resolution respirometry was performed using an OROBOROS® Oxygraph 2K (Innsbruck, Austria) as described previously (23). Respiration was started by the addition of palmitoylcarnitine (20 μM)/malate (5 mM), pyruvate (5 mM)/malate, or pyruvate/glutamate (10 mM)/malate (state 2) followed by sequential addition of ADP (1.25 mM) (state 3), succinate (5 mM) (state 3 Max), rotenone (0.5 μM), oligomycin (2.5 μM) (state 4), and antimycin A (3.75 μM). For measurement of ATP production, a 10-μl aliquot was collected from the respirometry chamber during state 3 respiration for 3 min following addition of ADP, mixed with an equal volume of DMSO, and stored at −80 °C for subsequent measurement of ATP synthesis using an ATP determination kit (Molecular Probes, Eugene, OR) according to the manufacturer's instructions. Finally, the ATP/O (P/O) ratio was determined by ATP production and O_2 consumption during state 3 respiration.

Mitochondrial Membrane Potentiometry—Mitochondrial membrane potential ($\Delta\Psi_{mt}$) measurement was performed using OROBOROS® Oxygraph 2K equipped with a TPP^+ ion-selective electrode. Mitochondria isolated from C57BL/6J mice (4–5 months of age) were placed into a chamber containing a buffer solution of 0.23 M mannitol, 0.07 M sucrose, 3 mM HEPES, pH 7.2, 5 mM succinate, and 2 μM TPP·Cl at 30 °C. 0.1 mM KH_2PO_4 and oxidized fatty acids (1 μM 12-HETE, 20-HETE,

14,15-EET, PGE_2, 9-oxoODE, or 8-HDoHE) or ethanol vehicle for control were added to the chamber. $CaCl_2$ was sequentially injected at 4-min intervals to 10, 20, 40, 60, and 80 μM final concentration. Mitochondrial membrane potential was calculated by following the instructions provided by the manufacturer (OROBOROS INSTRUMENTS Corp.).

Mitochondrial Swelling Assays—For determination of mPTP opening, isolated mitochondria from wild-type and CMiPLA$_2\gamma$KO mouse hearts were placed in mitochondrial swelling buffer (3 mM HEPES, pH 7.0, containing 0.23 M mannitol, 70 mM sucrose, 5 mM succinate, 1.25 μM rotenone, and 2 mM KH_2PO_4). 70 μg of mitochondria were placed in a 96-well plate with either ethanol vehicle alone (1%), 0.5 or 2 μM palmitic acid, and mitochondrial swelling was initiated by addition of 150 μM $CaCl_2$ (final) with comparisons with the addition of 10 μM EGTA as control. Decreases in absorbance (540 nm) are indicative of swelling of the mitochondria by opening of the mPTP and were monitored every 15 s using a SpectraMax M5e microplate reader (Molecular Devices, Sunnyvale, CA) (9).

Myocardial Ischemia Reperfusion Studies—The methods of Weinheimer *et al.* (60) were used. Mice were subjected to reversible left anterior descending (LAD) coronary artery occlusion to induce ischemia for 30 min, followed by 24 h of reperfusion. Briefly, mice were anesthetized with a mixture of ketamine (100 mg/kg of body weight) and xylazine (10 mg/kg), surgically prepped, and ventilated. After thoracotomy, the LAD artery was identified, and a 9-0 polypropylene suture was passed under the LAD artery. A knot was tied over a 1-mm section of PE-10 tubing placed directly over the vessel to create the occlusion. Ischemia was confirmed by an absence of blood flow and verified visually and by the presence of ST elevations on the electrocardiogram. The chest wall was approximated and covered with moistened gauze during the 30-min ischemia time. Reperfusion was induced by cutting the knot on top of the polyethylene tubing or simply removing the tubing piece. This allowed release of the occlusion, and resolution of ST segment elevations was observed. The chest was then closed, and mice were monitored closely for warmth and recovery until the end of the reperfusion time. After 24 h, the mice were given heparin (100 units, i.p.) and re-anesthetized with ketamine/xylazine, and the sternotomy was re-opened to expose the heart. The heart was excised and perfused retrograde through a catheter placed in the aorta. After slow perfusion of 1–2 ml of warmed phosphate-buffered saline (37 °C) to remove blood, the LAD was re-occluded with the 8-0 suture, and the heart was perfused with 5% Phthalo blue dye (Heucotech Ltd., Fairless Hill, PA) in saline to delineate the previously occluded and reperfused vascular bed (area-at-risk). The portion of the LV supplied by the occluded coronary was identified by the absence of blue dye. The heart was then wrapped in Saran wrap and placed in a −20 °C freezer for 10 min. The ventricles were then cut with a scalpel in 1–2-mm transverse sections, and the slices were photographed on both sides to identify the perfused myocardium. The slices were stained by immersion with 1% triphenyltetrazolium chloride (TTC) (in phosphate buffer, pH 7.4, 37 °C), which forms an insoluble red diformazan product in the presence of active dehydrogenase enzymes. The slices were weighed and re-photographed at low magnification on both sides. The images from dye perfusion (area-at-risk) and TTC staining were digitized to permit computerized videoplanimetry of TTC stained and unstained tissue as well as the area perfused and non-perfused with Phthalo dye on the surface of each slice. The percentage of the surface area-at-risk that was infarcted was averaged for each group of mice, and the degree of infarction was calculated as a percentage of the area-at-risk.

Miscellaneous Procedures—Standard methods were used for SDS-PAGE and Western analyses. Protein concentration was measured by a Bradford assay (Bio-Rad) or bicinchoninic acid assay (Thermo Scientific) utilizing bovine serum albumin as standard. Northern and Southern analyses were performed as described previously (22).

Statistics—Comparisons between the WT and CMiPLA$_2\gamma$KO groups studied were made using a two-tailed Student's *t* test. A value of $p < 0.05$ was considered significant. All data are reported as the means ± S.E. unless otherwise noted.

Author Contributions—S. H. M., D. J. M., and R. W. G. designed studies. D. J. M., S. G., and H. F. S. generated and provided cardiac myocyte-specific iPLA$_2\gamma$ knock-out mice. C. J. W. performed the mouse *in vivo* ischemia/reperfusion survival surgery experiments. A. L. N. and D. A. performed *ex vivo* tissue perfusion studies and infarct sizing. A. K. performed echocardiographic analyses of mouse myocardial hemodynamic function. X. L. and K. Y. performed mass spectrometric analyses of lipids. S. H. M., D. J. M., H. F. S., B. G. D., and C. M. J. conducted the experiments and analyzed the data in conjunction with R. W. G. This manuscript was prepared by S. H. M., C. M. J., and R. W. G.

Acknowledgments—We acknowledge the services provided by the Mouse Genetics Core and the Mouse Cardiovascular Phenotyping Core at Washington University.

References

1. Bagai, A., Dangas, G. D., Stone, G. W., and Granger, C. B. (2014) Reperfusion strategies in acute coronary syndromes. *Circ. Res.* **114,** 1918–1928
2. Sluijter, J. P., Condorelli, G., Davidson, S. M., Engel, F. B., Ferdinandy, P., Hausenloy, D. J., Lecour, S., Madonna, R., Ovize, M., Ruiz-Meana, M., Schulz, R., Van Laake, L. W., Nucleus of the European Society of Cardiology Working Group Cellular Biology of the Heart. (2014) Novel therapeutic strategies for cardioprotection. *Pharmacol. Ther.* **144,** 60–70
3. Reddy, K., Khaliq, A., and Henning, R. J. (2015) Recent advances in the diagnosis and treatment of acute myocardial infarction. *World J. Cardiol.* **7,** 243–276
4. Hausenloy, D. J., and Yellon, D. M. (2013) Myocardial ischemia-reperfusion injury: a neglected therapeutic target. *J. Clin. Invest.* **123,** 92–100
5. Yellon, D. M., and Hausenloy, D. J. (2007) Myocardial reperfusion injury. *N. Engl. J. Med.* **357,** 1121–1135
6. Kwong, J. Q., and Molkentin, J. D. (2015) Physiological and pathological roles of the mitochondrial permeability transition pore in the heart. *Cell Metab.* **21,** 206–214
7. Halestrap, A. P., Clarke, S. J., and Javadov, S. A. (2004) Mitochondrial permeability transition pore opening during myocardial reperfusion–a target for cardioprotection. *Cardiovasc. Res.* **61,** 372–385
8. Morciano, G., Giorgi, C., Bonora, M., Punzetti, S., Pavasini, R., Wieckowski, M. R., Campo, G., and Pinton, P. (2015) Molecular identity of the mitochondrial permeability transition pore and its role in ischemia-reperfusion injury. *J. Mol. Cell. Cardiol.* **78,** 142–153
9. Moon, S. H., Jenkins, C. M., Kiebish, M. A., Sims, H. F., Mancuso, D. J., and Gross, R. W. (2012) Genetic ablation of calcium-independent phospholipase A2γ (iPLA2γ) attenuates calcium-induced opening of the mito-

chondrial permeability transition pore and resultant cytochrome c release. *J. Biol. Chem.* **287,** 29837–29850
10. Furuno, T., Kanno, T., Arita, K., Asami, M., Utsumi, T., Doi, Y., Inoue, M., and Utsumi, K. (2001) Roles of long chain fatty acids and carnitine in mitochondrial membrane permeability transition. *Biochem. Pharmacol.* **62,** 1037–1046
11. Wolkowicz, P. E., and McMillin-Wood, J. (1980) Dissociation between mitochondria calcium ion release and pyridine nucleotide oxidation. *J. Biol. Chem.* **255,** 10348–10353
12. Beatrice, M. C., Palmer, J. W., and Pfeiffer, D. R. (1980) The relationship between mitochondrial membrane permeability, membrane potential, and the retention of Ca^{2+} by mitochondria. *J. Biol. Chem.* **255,** 8663–8671
13. Mittnacht, S., Jr., and Farber, J. L. (1981) Reversal of ischemic mitochondrial dysfunction. *J. Biol. Chem.* **256,** 3199–3206
14. Wojtczak, L., and Wieckowski, M. R. (1999) The mechanisms of fatty acid-induced proton permeability of the inner mitochondrial membrane. *J. Bioenerg. Biomembr.* **31,** 447–455
15. Penzo, D., Petronilli, V., Angelin, A., Cusan, C., Colonna, R., Scorrano, L., Pagano, F., Prato, M., Di Lisa, F., and Bernardi, P. (2004) Arachidonic acid released by phospholipase A2 activation triggers Ca^{2+}-dependent apoptosis through the mitochondrial pathway. *J. Biol. Chem.* **279,** 25219–25225
16. Halestrap, A. P., and Richardson, A. P. (2015) The mitochondrial permeability transition: a current perspective on its identity and role in ischaemia/reperfusion injury. *J. Mol. Cell. Cardiol.* **78,** 129–141
17. Whelan, R. S., Konstantinidis, K., Wei, A. C., Chen, Y., Reyna, D. E., Jha, S., Yang, Y., Calvert, J. W., Lindsten, T., Thompson, C. B., Crow, M. T., Gavathiotis, E., Dorn, G. W., 2nd, O'Rourke, B., and Kitsis, R. N. (2012) Bax regulates primary necrosis through mitochondrial dynamics. *Proc. Natl. Acad. Sci. U.S.A.* **109,** 6566–6571
18. Mancuso, D. J., Jenkins, C. M., and Gross, R. W. (2000) The genomic organization, complete mRNA sequence, cloning, and expression of a novel human intracellular membrane-associated calcium-independent phospholipase A2. *J. Biol. Chem.* **275,** 9937–9945
19. Mancuso, D. J., Jenkins, C. M., Sims, H. F., Cohen, J. M., Yang, J., and Gross, R. W. (2004) Complex transcriptional and translational regulation of iPLA2γ resulting in multiple gene products containing dual competing sites for mitochondrial or peroxisomal localization. *Eur. J. Biochem.* **271,** 4709–4724
20. Mancuso, D. J., Han, X., Jenkins, C. M., Lehman, J. J., Sambandam, N., Sims, H. F., Yang, J., Yan, W., Yang, K., Green, K., Abendschein, D. R., Saffitz, J. E., and Gross, R. W. (2007) Dramatic accumulation of triglycerides and precipitation of cardiac hemodynamic dysfunction during brief caloric restriction in transgenic myocardium expressing human calcium-independent phospholipase A2γ. *J. Biol. Chem.* **282,** 9216–9227
21. Eaddy, A. C., Cummings, B. S., McHowat, J., and Schnellmann, R. G. (2012) The role of endoplasmic reticulum Ca^{2+}-independent phospholipase A2γ in oxidant-induced lipid peroxidation, Ca^{2+} release, and renal cell death. *Toxicol. Sci.* **128,** 544–552
22. Mancuso, D. J., Sims, H. F., Han, X., Jenkins, C. M., Guan, S. P., Yang, K., Moon, S. H., Pietka, T., Abumrad, N. A., Schlesinger, P. H., and Gross, R. W. (2007) Genetic ablation of calcium-independent phospholipase A2γ leads to alterations in mitochondrial lipid metabolism and function resulting in a deficient mitochondrial bioenergetic phenotype. *J. Biol. Chem.* **282,** 34611–34622
23. Mancuso, D. J., Sims, H. F., Yang, K., Kiebish, M. A., Su, X., Jenkins, C. M., Guan, S., Moon, S. H., Pietka, T., Nassir, F., Schappe, T., Moore, K., Han, X., Abumrad, N. A., and Gross, R. W. (2010) Genetic ablation of calcium-independent phospholipase A2γ prevents obesity and insulin resistance during high fat feeding by mitochondrial uncoupling and increased adipocyte fatty acid oxidation. *J. Biol. Chem.* **285,** 36495–36510
24. Mancuso, D. J., Kotzbauer, P., Wozniak, D. F., Sims, H. F., Jenkins, C. M., Guan, S., Han, X., Yang, K., Sun, G., Malik, I., Conyers, S., Green, K. G., Schmidt, R. E., and Gross, R. W. (2009) Genetic ablation of calcium-independent phospholipase A2γ leads to alterations in hippocampal cardiolipin content and molecular species distribution, mitochondrial degeneration, autophagy, and cognitive dysfunction. *J. Biol. Chem.* **284,** 35632–35644
25. Yan, W., Jenkins, C. M., Han, X., Mancuso, D. J., Sims, H. F., Yang, K., and Gross, R. W. (2005) The highly selective production of 2-arachidonoyl lysophosphatidylcholine catalyzed by purified calcium-independent phospholipase A2γ: identification of a novel enzymatic mediator for the generation of a key branch point intermediate in eicosanoid signaling. *J. Biol. Chem.* **280,** 26669–26679
26. Han, X., Yang, K., and Gross, R. W. (2012) Multi-dimensional mass spectrometry-based shotgun lipidomics and novel strategies for lipidomic analyses. *Mass Spectrom. Rev.* **31,** 134–178
27. Chicco, A. J., and Sparagna, G. C. (2007) Role of cardiolipin alterations in mitochondrial dysfunction and disease. *Am. J. Physiol. Cell Physiol.* **292,** C33–C44
28. Chicco, A. J., Sparagna, G. C., McCune, S. A., Johnson, C. A., Murphy, R. C., Bolden, D. A., Rees, M. L., Gardner, R. T., and Moore, R. L. (2008) Linoleate-rich high-fat diet decreases mortality in hypertensive heart failure rats compared with lard and low-fat diets. *Hypertension* **52,** 549–555
29. Kiebish, M. A., Yang, K., Sims, H. F., Jenkins, C. M., Liu, X., Mancuso, D. J., Zhao, Z., Guan, S., Abendschein, D. R., Han, X., and Gross, R. W. (2012) Myocardial regulation of lipidomic flux by cardiolipin synthase: setting the beat for bioenergetic efficiency. *J. Biol. Chem.* **287,** 25086–25097
30. Mulligan, C. M., Sparagna, G. C., Le, C. H., De Mooy, A. B., Routh, M. A., Holmes, M. G., Hickson-Bick, D. L., Zarini, S., Murphy, R. C., Xu, F. Y., Hatch, G. M., McCune, S. A., Moore, R. L., and Chicco, A. J. (2012) Dietary linoleate preserves cardiolipin and attenuates mitochondrial dysfunction in the failing rat heart. *Cardiovasc. Res.* **94,** 460–468
31. Han, X., Yang, K., Yang, J., Cheng, H., and Gross, R. W. (2006) Shotgun lipidomics of cardiolipin molecular species in lipid extracts of biological samples. *J. Lipid Res.* **47,** 864–879
32. Yoda, E., Hachisu, K., Taketomi, Y., Yoshida, K., Nakamura, M., Ikeda, K., Taguchi, R., Nakatani, Y., Kuwata, H., Murakami, M., Kudo, I., and Hara, S. (2010) Mitochondrial dysfunction and reduced prostaglandin synthesis in skeletal muscle of Group VIB Ca^{2+}-independent phospholipase A2γ-deficient mice. *J. Lipid Res.* **51,** 3003–3015
33. Sharma, J., and McHowat, J. (2011) PGE2 release from tryptase-stimulated rabbit ventricular myocytes is mediated by calcium-independent phospholipase A2γ. *Lipids* **46,** 391–397
34. Moon, S. H., Jenkins, C. M., Liu, X., Guan, S., Mancuso, D. J., and Gross, R. W. (2012) Activation of mitochondrial calcium-independent phospholipase A2γ (iPLA2γ) by divalent cations mediating arachidonate release and production of downstream eicosanoids. *J. Biol. Chem.* **287,** 14880–14895
35. Elimam, H., Papillon, J., Takano, T., and Cybulsky, A. V. (2013) Complement-mediated activation of calcium-independent phospholipase A2γ: role of protein kinases and phosphorylation. *J. Biol. Chem.* **288,** 3871–3885
36. Liu, X., Moon, S. H., Mancuso, D. J., Jenkins, C. M., Guan, S., Sims, H. F., and Gross, R. W. (2013) Oxidized fatty acid analysis by charge-switch derivatization, selected reaction monitoring, and accurate mass quantitation. *Anal. Biochem.* **442,** 40–50
37. Unger, R. H., and Orci, L. (2002) Lipoapoptosis: its mechanism and its diseases. *Biochim. Biophys. Acta* **1585,** 202–212
38. Ong, S. B., Samangouei, P., Kalkhoran, S. B., and Hausenloy, D. J. (2015) The mitochondrial permeability transition pore and its role in myocardial ischemia reperfusion injury. *J. Mol. Cell. Cardiol.* **78,** 23–34
39. Idell-Wenger, J. A., Grotyohann, L. W., and Neely, J. R. (1978) Coenzyme A and carnitine distribution in normal and ischemic hearts. *J. Biol. Chem.* **253,** 4310–4318
40. Goñi, F. M., Requero, M. A., and Alonso, A. (1996) Palmitoylcarnitine, a surface-active metabolite. *FEBS Lett.* **390,** 1–5
41. Petronilli, V., Penzo, D., Scorrano, L., Bernardi, P., and Di Lisa, F. (2001) The mitochondrial permeability transition, release of cytochrome c and cell death. Correlation with the duration of pore openings *in situ*. *J. Biol. Chem.* **276,** 12030–12034
42. Rauckhorst, A. J., Pfeiffer, D. R., and Broekemeier, K. M. (2015) The iPLA2γ is identified as the membrane potential sensitive phospholipase in liver mitochondria. *FEBS Lett.* **589,** 2367–2371
43. Haworth, R. A., Potter, K. T., and Russell, D. C. (2010) Role of arachidonic

acid, lipoxygenase, and mitochondrial depolarization in reperfusion arrhythmias. *Am. J. Physiol. Heart Circ. Physiol.* **299,** H165–H174
44. Nazarewicz, R. R., Zenebe, W. J., Parihar, A., Parihar, M. S., Vaccaro, M., Rink, C., Sen, C. K., and Ghafourifar, P. (2007) 12(*S*)-hydroperoxyeicosatetraenoic acid (12-HETE) increases mitochondrial nitric oxide by increasing intramitochondrial calcium. *Arch. Biochem. Biophys.* **468,** 114–120
45. Serhan, C. N., Chiang, N., and Van Dyke, T. E. (2008) Resolving inflammation: dual anti-inflammatory and pro-resolution lipid mediators. *Nat. Rev. Immunol.* **8,** 349–361
46. Danial, N. N., and Korsmeyer, S. J. (2004) Cell death: critical control points. *Cell* **116,** 205–219
47. Xu, S., Nam, S. M., Kim, J. H., Das, R., Choi, S. K., Nguyen, T. T., Quan, X., Choi, S. J., Chung, C. H., Lee, E. Y., Lee, I. K., Wiederkehr, A., Wollheim, C. B., Cha, S. K., and Park, K. S. (2015) Palmitate induces ER calcium depletion and apoptosis in mouse podocytes subsequent to mitochondrial oxidative stress. *Cell Death Dis.* **6,** e1976
48. Fauconnier, J., Andersson, D. C., Zhang, S. J., Lanner, J. T., Wibom, R., Katz, A., Bruton, J. D., and Westerblad, H. (2007) Effects of palmitate on Ca^{2+} handling in adult control and ob/ob cardiomyocytes: impact of mitochondrial reactive oxygen species. *Diabetes* **56,** 1136–1142
49. Fang, K. M., Lee, A. S., Su, M. J., Lin, C. L., Chien, C. L., and Wu, M. L. (2008) Free fatty acids act as endogenous ionophores, resulting in Na^+ and Ca^{2+} influx and myocyte apoptosis. *Cardiovasc. Res.* **78,** 533–545
50. Jenkins, C. M., Cedars, A., and Gross, R. W. (2009) Eicosanoid signalling pathways in the heart. *Cardiovasc. Res.* **82,** 240–249
51. Gabbs, M., Leng, S., Devassy, J. G., Monirujjaman, M., and Aukema, H. M. (2015) Advances in our understanding of oxylipins derived from dietary PUFAs. *Adv. Nutr.* **6,** 513–540
52. Song, L., Yang, H., Wang, H. X., Tian, C., Liu, Y., Zeng, X. J., Gao, E., Kang, Y. M., Du, J., and Li, H. H. (2014) Inhibition of 12/15 lipoxygenase by baicalein reduces myocardial ischemia/reperfusion injury via modulation of multiple signaling pathways. *Apoptosis* **19,** 567–580
53. Han, Y., Zhao, H., Tang, H., Li, X., Tan, J., Zeng, Q., and Sun, C. (2013) 20-Hydroxyeicosatetraenoic acid mediates isolated heart ischemia/reperfusion injury by increasing NADPH oxidase-derived reactive oxygen species production. *Circ. J.* **77,** 1807–1816
54. Xu, Y. J., Ho, W. E., Xu, F., Wen, T., and Ong, C. N. (2013) Exploratory investigation reveals parallel alteration of plasma fatty acids and eicosanoids in coronary artery disease patients. *Prostaglandins Other Lipid Mediat.* **106,** 29–36
55. Ma, Y., Zhang, P., Li, J., Lu, J., Ge, J., Zhao, Z., Ma, X., Wan, S., Yao, X., and Shen, B. (2015) Epoxyeicosatrienoic acids act through TRPV4-TRPC1-KCa1.1 complex to induce smooth muscle membrane hyperpolarization and relaxation in human internal mammary arteries. *Biochim. Biophys. Acta* **1852,** 552–559
56. Kacik, M., Oliván-Viguera, A., and Köhler, R. (2014) Modulation of K(Ca)3.1 channels by eicosanoids, ω-3 fatty acids, and molecular determinants. *PLoS ONE* **9,** e112081
57. Tanaka, N., Dalton, N., Mao, L., Rockman, H. A., Peterson, K. L., Gottshall, K. R., Hunter, J. J., Chien, K. R., and Ross, J., Jr. (1996) Transthoracic echocardiography in models of cardiac disease in the mouse. *Circulation* **94,** 1109–1117
58. Rockman, H. A., Chien, K. R., Choi, D. J., Iaccarino, G., Hunter, J. J., Ross, J., Jr., Lefkowitz, R. J., and Koch, W. J. (1998) Expression of a β-adrenergic receptor kinase 1 inhibitor prevents the development of myocardial failure in gene-targeted mice. *Proc. Natl. Acad. Sci. U.S.A.* **95,** 7000–7005
59. Han, X., Yang, J., Cheng, H., Yang, K., Abendschein, D. R., and Gross, R. W. (2005) Shotgun lipidomics identifies cardiolipin depletion in diabetic myocardium linking altered substrate utilization with mitochondrial dysfunction. *Biochemistry* **44,** 16684–16694
60. Ma, X., Liu, H., Murphy, J. T., Foyil, S. R., Godar, R. J., Abuirqeba, H., Weinheimer, C. J., Barger, P. M., and Diwan, A. (2015) Regulation of the transcription factor EB-PGC1α axis by beclin-1 controls mitochondrial quality and cardiomyocyte death under stress. *Mol. Cell. Biol.* **35,** 956–976